

## 키토산/카프로락탐 혼합체에 대한 수분의 영향\*

리아오셴-쿤 · 흥치치<sup>†</sup> · 린망퐁\*\*

펑치아대학 교 섬유복합재료학과, 대만 타이중시, \*\*국제기술연구소 경영행정학과, 대만 윤린시  
(2004년 6월 9일 접수, 2004년 9월 20일 채택)

### Effect of Moisture on Molecular Motions of Chitosan/Polycaprolactam Blends

Shen-Kun Liao, Chi-Chih Hung<sup>†</sup>, and Ming-Fung Lin\*\*

Department of Fiber and Composite Materials, Feng Chia University, Taichung, Taiwan

\*\*Department of Business & Administration Management,  
Transworld Institute of Technology, Yunlin, Taiwan

<sup>†</sup>e-mail : chichih@seed.net.tw

(Received June 9, 2004; accepted September 20, 2004)

**초록 :** 키토산과 폴리카프로락탐 (PA6) 복합체의 박막을 박막을 개미산을 사용하여 만들었다. FT-IR 분광학적 자료는 키토산의 히드록시기와 PA6의 아마이드기 사이의 수소 결합이 형성되었음을 보여주었다. 열무게분석법은 혼합체 시료는 수분을 포함하고 있음을 나타내었다. 시료 속의 물의 분산은 저장 탄성률 ( $E'$ )을 크게 감소한다고 DMA 결과는 보여주었다. 혼합체 시료의 기계적 손실 탄젠트 ( $\tan \delta$ ) 자료는  $\beta$ d 손실 피크가 0 °C 부근에서 나타남을 보여주었다. 혼합체 시료들은 진공에서 완전히 건조하였고 그다음 소위 w-다리를 만드는 물을 흡수할 수 있도록 높은 습도 속에 두었다. 이 시료들의  $E'$  자료는 비정상적으로 증가하였고 50 °C 부근에서 손실 피크의 어깨에 추가적인 손실 피크가 나타났다. 건조한 조건하에서는, 40/60 혼합 비율의 키토산/PA6가 두 성분의 섞임성이 더 좋았다.

**ABSTRACT :** The membranes of the blends of chitosan and polycaprolactam (PA6) were prepared in formic acid. FT-IR data revealed that hydrogen bonding between amide and hydroxyl groups of chitosan and PA6, respectively, was formed. Thermogravimetric analysis demonstrated that the blend samples contain water. DMA results showed that the dissipation of water in the samples significantly reduced the storage modulus ( $E'$ ). The mechanical loss tangent ( $\tan \delta$ ) data of the blend samples showed the  $\beta$ d loss peak around 0 °C. The blend samples were completely dried in a vacuum and then exposed to high moisture to absorb water which would cause, so called, w-bridges between the molecules. The  $E'$  data of these regained samples increased abnormally and additional loss peak appeared on the shoulder of the peak around 50 °C. Under dry condition, the samples with a blend ratio of 40/60 for chitosan/PA6 displayed a better miscibility between two components.

**Keywords :** blend, chitosan, polycaprolactam, hydrogen bond, miscibility.

### 1. Introduction

Polymer blending generally aims to improve polymer characteristics and increase its applications.<sup>1</sup> Natural polymer such as polysaccharide has the advantage of biodegradability, but its

molecular weight is unevenly distributed and its mechanical properties are generally poor. In contrast, synthetic polymer can have evenly distributed molecular weight and mechanical properties superior to those of natural but polymer depending on the polymerization condition, but the synthetic polymer is

\*: The title, names of authors, addresses, and abstract in English were translated into Korean by the editor under an agreement with the corresponding author.

usually known to be non-biodegradable. Blended natural polymer with synthetic polymer, called bio-polymer, combines good mechanical properties with biodegradability, increasing its economic benefits.<sup>2</sup> Recently, some researchers have focused on blending polymers, for example blending cellulose with poly(vinyl pyrrolidone), polyamide, polyacrylonitrile and poly(vinyl alcohol), and studying their phase behavior, morphology, mechanical properties, permeation and adsorption properties of these blends.<sup>3-8</sup>

Chitin is a biodegradable polymer with the main chain structure ( $\beta$ -(1-4)D-glucopyranose) like cellulose. The crucial difference is that, in the C-2 position, the hydroxyl is replaced by the acetamide and forms [ $\beta$ -(1-4)-2-acetamido-2-deoxy-]-D-glucopyranose], which is the major structure of chitin. Chitosan is obtained through deacetylating chitin,<sup>9-11</sup> but the chitin is difficult to be deacetylated completely. The chitosan is classified into several types based on its molecular weights and deacetylation. Figure 1 illustrates the structures of cellulose, chitin and chitosan, respectively. Over 80% deacetylation materials are intended for commercial applications with some acetyl residues; thus, chitosan is a kind of heteropolymers.<sup>12-17</sup>

Since chitosan contains cations, it can suppress growth of micro-organisms and bacteria that possess anions. However, its applications involving face difficulties owing to its weak mechanical properties. Therefore, blending with different polymers is one way of improving those weak mechanical properties of chitosan. In the polymer selection, chemical or physical similarities among compositions increase miscibility, while the formation of secondary bonds (such as hydrogen-bonds and van der Waals force) also increases miscibility. Polycaprolactam (PA6, structure shown in Figure 2) and chitosan have strong polarity groups and form strong hydrogen bonds. Adopting PA6 as the second composition blended with chitosan can improve mechanical properties and increase applications of chitosan.

Compatibility affecting the mechanical properties is a key factor in polymer blending, and blend miscibility can be evaluated by measuring the glass transition temperature ( $T_g$ ). Supposedly, blends with fine miscibility typically have only one glass transition temperature, and otherwise have an individual glass transition temperature. Differential scanning calorimetry (DSC) can be used to measure the glass transition temperature of polymer and determine blend miscibility. However, this method is ineffective for evaluating the miscibility of blend because its glass transition temperature is not mani-

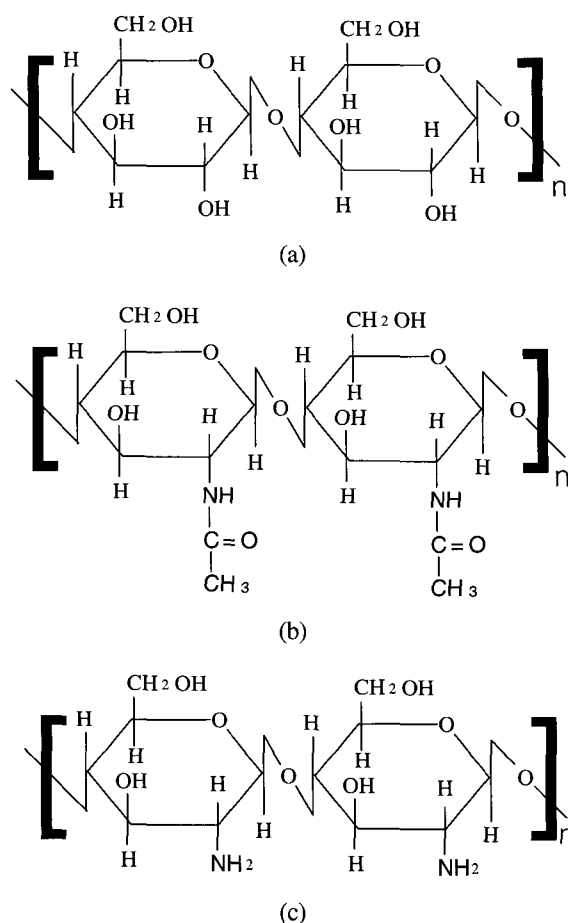


Figure 1. Chemical structure of (a) cellulose, (b) chitin and (c) chitosan.

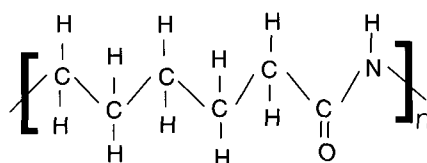


Figure 2. Chemical structure of polycaprolactam (PA6).

fest.<sup>18</sup> Nevertheless, dynamic mechanical analysis and dielectric spectroscopy analysis offer other approaches for measuring glass transition temperature, molecular motion and relaxation. The two methods are successfully applied to various types of carbohydrate polymers to observe the molecular motion and miscibility.<sup>19-24</sup> Relevant research using a DMA measurement found that moisture affects the modulus changes and mechanical loss tangent of the hydrophilic polymers (such as cellulose).<sup>19</sup> However, detailed discussion is lacking on the moisture contained in and removed from chitosan, and the

**Table 1. Blend Ratios of the Samples**

| sample code      | chitosan | PA6-10% | PA6-20% | PA6-30% | PA6-40% | PA6-50% | PA6-60% | PA6-70% | PA6-80% | PA6-90% | PA6     |
|------------------|----------|---------|---------|---------|---------|---------|---------|---------|---------|---------|---------|
| chitosan content | 100 wt%  | 90 wt%  | 80 wt%  | 70 wt%  | 60 wt%  | 50 wt%  | 40 wt%  | 30 wt%  | 20 wt%  | 10 wt%  | 0 wt%   |
| PA6 content      | 0 wt%    | 10 wt%  | 20 wt%  | 30 wt%  | 40 wt%  | 50 wt%  | 60 wt%  | 70 wt%  | 80 wt%  | 90 wt%  | 100 wt% |

relations among molecular motion, modulus changes and miscibility in DMA measurement.

This investigation first uses an FT-IR to observe the effect of hydrogen bond between chitosan and PA6, and uses the TGA to measure the thermal degradation of individual chitosan/PA6 blended sample. Simultaneously, the results of DMA are utilized to evaluate the molecular motion, modulus changes and miscibility of blends containing moisture and dehydrate. Based on the results of DMA, we obtain an optimum blending ratio of chitosan/PA6 blended samples.

## 2. Experimental

**Materials.** Polycaprolactam with an weight average molecular weight ( $M_w$ ) of  $3.0 \times 10^4$  was purchased from Aldrich USA, Co. USA, and 84.5% deacetylated chitosan with  $M_w = 1.5 \times 10^5$  was obtained from Fluka Co., Swiss. Formic acid with 99% purity was purchased from Acros Co., USA.

**Preparation of Membrane.** The chitosan and polycaprolactam were dissolved in formic acid during the blending, and then heated at 65 °C for 4 h. Blending ratios of the polycaprolactam varied from 10% to 90% (wt%). The blended solution was spread on a glass plate, and then heated in a vacuum oven forming an approximately 0.07~0.15 mm thick membrane. The membrane was placed in a 2M sodium hydroxide solution for neutralization, then soaked in deionized water for 24 h, settled at room temperature and dried naturally. Table 1 lists the blending ratios and sample codes for each sample.

**Measurement.** FT-IR measurements with dried samples were taken using a PIKE 6141 spectrophotometer; and scanned ten times ranging from 500 to 4500  $\text{cm}^{-1}$  at room temperature. TGA measurements were conducted using Perkin Elmer TGA 1, with a sample weight of approximately 5 mg, a heating rate of 10 °C/min. The samples were tested in the nitrogen gas condition with a temperature ranging from 30 to 750 °C.

DSC measurements were taken using a Perkin Elmer Pyris 1 DSC, on samples with mass of about 5 mg, at heating rate of 10 °C/min; samples were tested in the nitrogen gas condition,

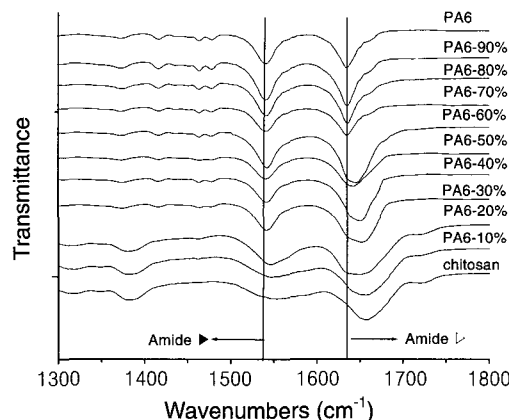


**Figure 3.** FT-IR spectra of chitosan/PA6 blended membranes.

and testing temperature ranging from 30 to 275 °C.

The DMA measurements were conducted using a Perkin Elmer DMA 7e, with a heating rate of 5 °C/min, a temperature ranging from -150 to 150 °C and a frequency of 1 Hz. Sample testing was conducted in two conditions of dry nitrogen gas filling and no gas filling. Moreover, the dimension of the testing sample was with a thickness of 0.07~0.15 mm, width of 5 mm and length of 10 mm. Two different testing samples were used, that is, one part of untreated samples and the other part samples were dehydrated at 100 °C for 10 min.

## 3. Results and Discussion

**FT-IR.** Figure 3 shows the FT-IR spectra of chitosan, PA6 and chitosan/PA6 blended samples, showing the absorption peak strength and frequency of amide group. The peak strength and frequency display the characteristics of transition, indicating a certain interaction between PA6 and chitosan. The amide I absorption peak of chitosan appears at 1657  $\text{cm}^{-1}$  while that of PA6 appears at 1632  $\text{cm}^{-1}$  as shown in Figure 3. In the amide II band, the absorption peak of chitosan appears at 1557  $\text{cm}^{-1}$  and that of PA6 presents at 1541  $\text{cm}^{-1}$ . For blended samples, the amide I absorption peak frequency of chitosan shifts to low frequency as the increasing of PA6 content and the maximum shift is approximately 25  $\text{cm}^{-1}$ . Similarly, the transition in the amide II band exhibits the same trend, but the frequency shift in the amide II band is less significant than that in the amide I

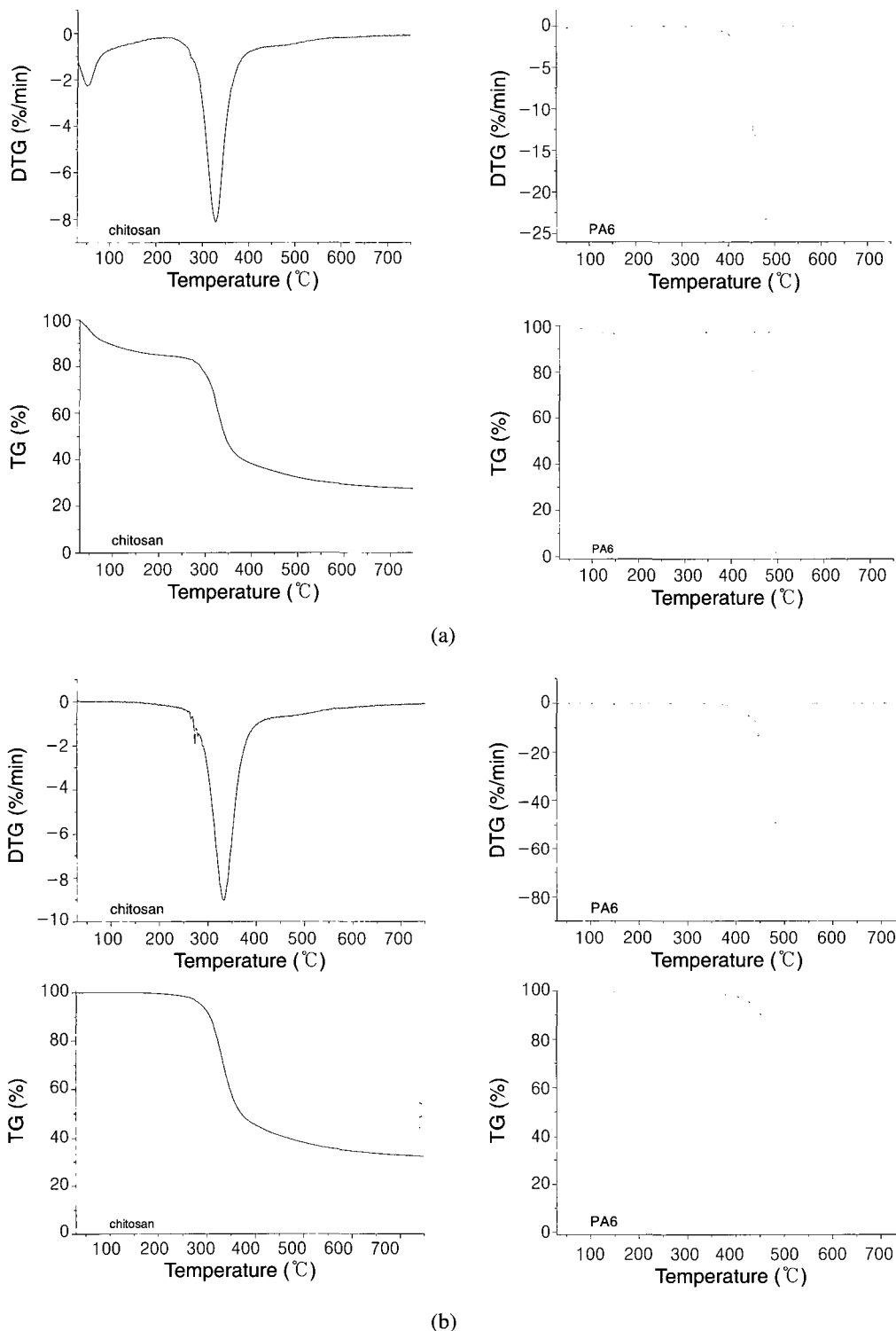


**Figure 4.** (a) TG and DTG curves of wet chitosan and wet PA6 obtained at a heating rate of 10 °C/min in an atmosphere of nitrogen, (b) TG and DTG curves of dry chitosan and dry PA6 obtained at a heating rate of 10 °C/min in an atmosphere of nitrogen.

band. Generally, the absorption peaks in the amide I and amide II bands shift toward a low frequency and no new absorption

peak is observed with varying PA6 content, demonstrating the formation of the hydrogen bond between chitosan and PA6.<sup>4,17,25</sup>

**TGA.**

**Degradation of Wet Samples :** Since both chitosan and polycaprolactam (PA6) possess polar groups, the water can be easily adsorbed onto the polymers by hydrogen bond. 26-29 As the temperature increases from 30 to 120 °C, the TG curve indicates 12 wt% weight loss of chitosan, implying the presence of water; this weight loss of PA6 is about 4 wt%, as indicated in Figures 4(a). Following the loss of water, chitosan and PA6 undergo a primary stage of degradation. The initial degradation temperature of chitosan is about 295 °C and its carbonization temperature is around 720 °C. The degradation temperature of PA6 is 437~510 °C. In spite of the water loss, the TG curves indicate that both polymers undergo a single stage of degradation.

For the chitosan and PA6 polymers being dried at 100 °C for 10 min, the TG curves indicate no weight loss of water, as shown in Figure 4(b). In subsequent experiments, all samples were dried at 100 °C for 10 min to proceed thermal degradation and measure weight loss. Moreover, the dry samples were very useful in thermogravimetric analysis.

**Degradation of Chitosan and PA 6 :** The TG curve of dry PA6 in Figure 4(b) has a horizontal baseline between 100 and 300 °C, implying completely dehydrated. However, the baseline of the TG curve for dry chitosan indicates 5 wt% weight loss between 100 and 280 °C, as shown in Figure 4(b); this weight loss is associated with deacetylation.<sup>30</sup>

The dry chitosan and PA6 exhibit a single stage of degradation and reflect a temperature of the maximum rate of degradation (DTG curve) as shown in Figure 4(b). The initial degradation temperature of chitosan is about 287 °C and its temperature of the maximum rate of degradation is about 313 °C. Finally, a high char residue of about 37 wt% is produced at 720 °C. The degradation of chitosan in fact starts with the amine groups and forms an unsaturated structure.<sup>30</sup> Similarly, PA6 also exhibits an initial degradation temperature at 429 °C and a temperature of maximum rate of degradation about 466 °C. The degradation of PA6 is related to the breakage of the main chain and depolymerization (a reversed reaction of cyclic polycondensation) to form a caprolactam;<sup>31,32</sup> finally, formed the char residual less than 0.21 wt%.

**Degradation of Chitosan Blended with PA6 :** These un-dehydrate chitosan/PA6 blended samples also exhibit various weight loss between 30 and 120 °C, as shown in Figure 5(a).

TGA is used herein to examine various components of blended samples. For these dried chitosan/PA6 blended sam-

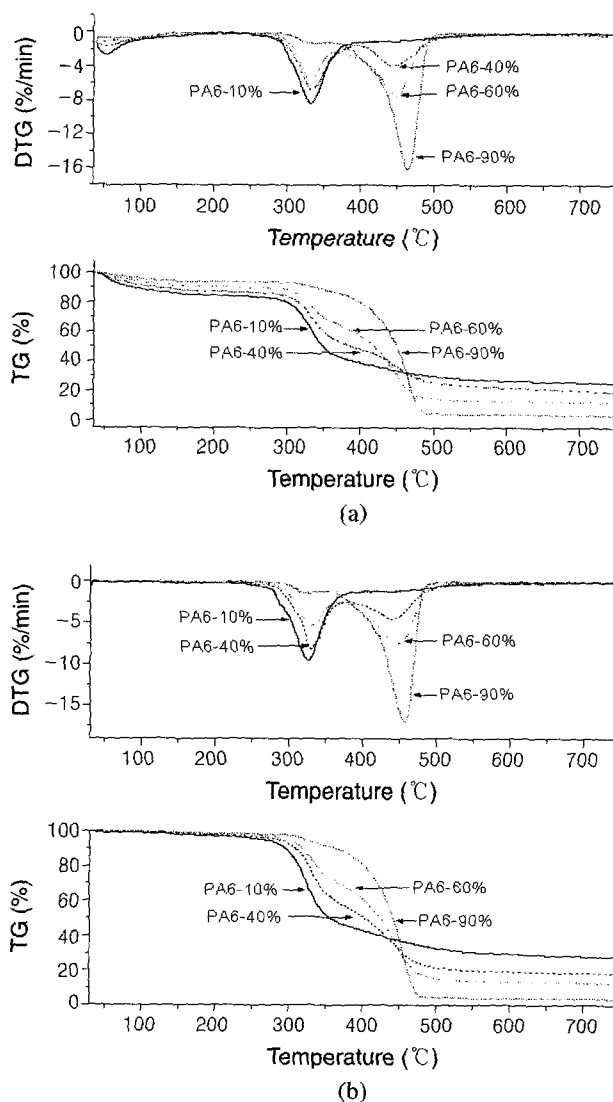


**Figure 5.** (a) TG and DTG curves of wet chitosan/PA6 of various proportions, obtained at a heating rate of 10 °C/min in an atmosphere of nitrogen atmosphere, (b) TG and DTG curves of dry chitosan/PA6 of various proportions, obtained at a heating rate of 10 °C/min in an atmosphere of nitrogen atmosphere.

ples, the degradation temperature ranges of the first and second stages seem to correspond to the degradation temperature ranges of pure chitosan and PA6, respectively. The two peaks on the DTG curves indicate the temperature of the maximum rate of the first and second degradation stages. However, the second stage of the blended samples that contains more than 30 wt% PA6 shift toward higher temperature, as shown in Figure 5(b). For blended samples, the degraded substrates of chitosan seem to affect the PA6 degradation earlier.

**DSC.** Figure 6(a) shows DSC scan of the chitosan. An

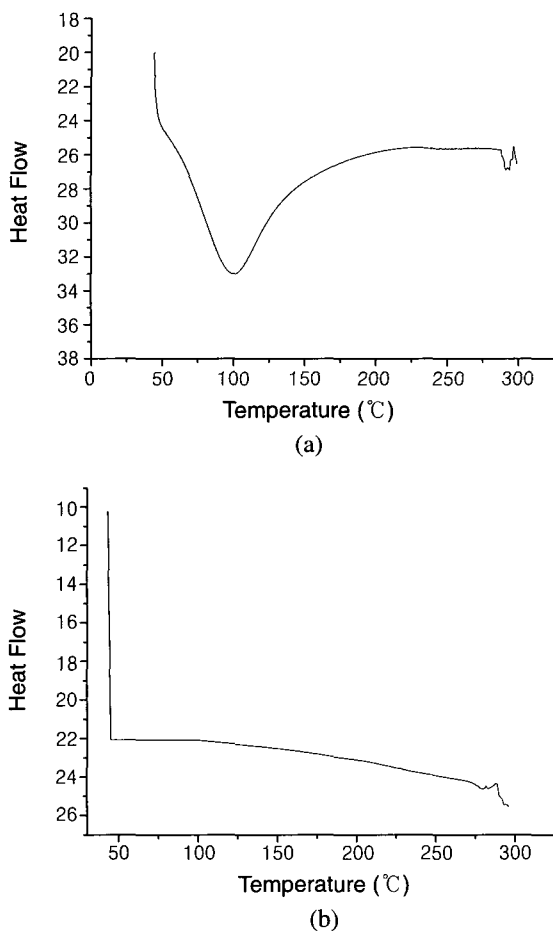


**Figure 6.** (a) DSC curve of wet chitosan obtained at a heating rate of 10 °C/min in an atmosphere of nitrogen, (b) DSC curve of dry chitosan obtained at a heating rate of 10 °C/min in an atmosphere of nitrogen.

endothermic peak centered on 100 °C can be assigned to the evaporation of adsorbed water. The sample stays at 100 °C for 10 min and cools down to room temperature, and then DSC scan starts. We do not find the endothermic peak on DSC curve (as shown in Figure 6(b)). The DSC curve of chitosan does not indicate any endothermic transition between room temperature and 250 °C that assigns the lack of any crystalline or any other phase change during the heating process. Sreenivasan<sup>18</sup> suggested that the strong endothermic peak around 270 °C was due to the oxidative degradation of chitosan. Thus, the endothermic peak centered around 287 °C in Figure 6(b) ought to the thermal degradation of the sample.

Figure 7 displays DSC scan of PA6 and chitosan/PA6 blended samples. The endothermic peak of adsorbed water evaporation disappears. We observe only one endothermic peak on each

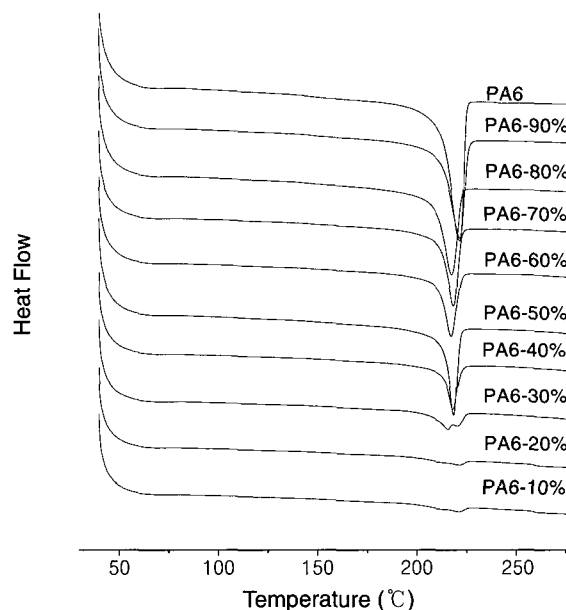


**Figure 7.** DSC curves of PA6 and chitosan/PA6 blended samples obtained at a heating rate of 10 °C/min in an atmosphere of nitrogen.

blended samples and the temperature of the endothermic peak corresponds to the  $T_m$  of PA6. Before the endothermic peak of  $T_m$ , no any slope change is observed. It was probably unavailable to examine the  $T_g$  of samples under DSC scan condition.

Basically, the temperature of endothermic peak shifts toward a low temperature with an increase of chitosan content. Above-mentioned results can be used to explain chitosan interfere the crystallization of PA6, both in reducing the size of crystalline and broadening the distribution of crystalline. The hydrogen bond formed between chitosan and PA6 molecular chains restricts the crystallization of PA6. Besides, the steric hindrance formed by the molecular chains of chitosan also restricts the movement of PA6 chains, and then causes the difficulties of crystallization. If the former effect plays as the main reason, a miscibility between chitosan and PA6 is regarded to be found. Because DSC results can't be used to evaluate the miscibility of chitosan/PA6 blended samples precisely, further evaluations for the same miscibility by DMA will be discussed in the next part.

#### Dynamic Mechanical Properties Analysis.

**Modulus and Chain Motion of Wet Sample :** Figure 8 illustrates the relationship between the storage modulus ( $E'$ ) and temperature of the wet sample. The modulus of some samples (as chitosan and PA6-10%) between -150 and 0 °C rapidly drop because of the moisture and molecular motion,

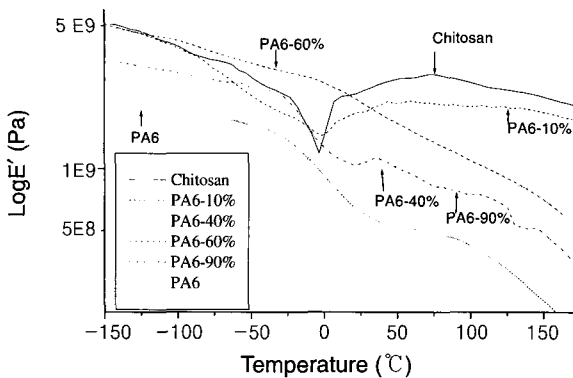


Figure 8. Storage modulus ( $\log E'$ ) of "wet" samples.

causing modulus loss.<sup>24</sup> As the temperature beyond 0 °C, however, the moduli of blended samples with low PA6 content (for example chitosan and PA6-10%) increase significantly. The result can be attributable to the heat promoted the scale of motion in the molecular chains; therefore, the polymer free volume is increased. Meanwhile, the heat effects increase the mobility of the water molecule. The water molecule easily enters into the free volume and links consecutively to each other. Finally, they connect the molecular chains and form cross-linkages (namely water-water bridge, w-bridge). Furthermore, the bonding force of these w-bridge occasionally is higher than that of the second bond of the polymer itself, thus increasing the modulus.<sup>33</sup> Similar observations have been reported for nylon by Prevorsek,<sup>34</sup> and for PVA by Takayanagi.<sup>35</sup> Prevorsek suggested that the water increased modulus by reducing free volume and formed the hydrogen bond (w-bridge) between the molecular chains. Nevertheless, the modulus declines as the temperature exceeds 70 °C due to the removing of moisture from samples.<sup>19</sup> PA6-40% and PA6-60% blended samples differ from the other samples. Their moduli continue to decline even though the temperature exceeds 0 °C. Probably, the samples in these two ratios have greater miscibility than the other ratios, so no extra water molecule exists between the chitosan and PA6 to form the w-bridge. The moisture thus probably only fills the voids and does not enter the molecular chain.

Figure 9 illustrates the relationship between dynamic loss tangent ( $\tan \delta$ ) and temperature. PA6 has three loss peaks ( $\gamma$ ,  $\beta$ ,  $\alpha$  peaks) from low to high temperatures, representing the motion of the methylene group between the amide groups, the partial motion of the amide group and the segment motion of the main chain, respectively. The  $\gamma$ ,  $\beta$ , and  $\alpha$  peaks appear at approximately -110, -76 and 70 °C, respectively. Chitosan has

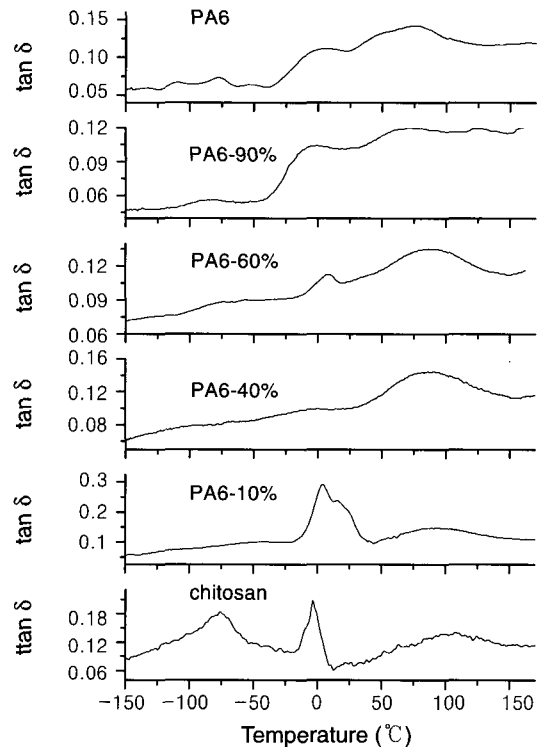


Figure 9. Loss tangent ( $\tan \delta$ ) of "wet" samples.

two loss peaks ( $\gamma$  and  $\alpha$  peaks). The  $\gamma$  peak occurs at -75 °C, resulting from vibrations of the polysaccharide, and  $\alpha$  peak is approximately 100 °C. Additionally, chitosan and PA6 give a peak around 0 °C individually, termed the  $\beta\delta$  peak. This loss peak assigns to moisture dissipation.<sup>19,33,36</sup>  $\beta\delta$  peak also is shown in the other blends. However, the  $\beta\delta$  peak is not observed in PA6-40% because the compact arrangement of molecular chains in this blend ratio is harmful to the forming of w-bridge between chitosan and PA6, indicating that this blend is likely to have good miscibility.

From Figure 9, chitosan has a large loss peak below 0 °C because chitosan has high crystallization and strong polarity, allowing the intermolecules to easily form network structures by hydrogen bond. Besides, the w-bridge makes the motion of chitosan segments difficult beneath 0 °C. Therefore, this loss peak is wide, like for the rigid polymers. However, after adding PA6, the PA6 soft segment fills into the space among the chitosan molecular chain and weakens the hydrogen bond effect between molecules and moisture. Meantime, PA6 soft segment also reduces the intra-molecular hydrogen bond in chitosan and form hydrogen bond with chitosan molecular chains. In turn, it enhances the motion ability of molecular chain, causing the reduction of  $\gamma$  peak in chitosan. Additionally,

the  $\gamma$  peak of PA6 is absent in the all blended samples. This phenomenon results from the effects of hydrogen bond and w-bridge. They restrict the motion of the methylene group, causing the  $\gamma$  peak of PA6 to diminish or even disappear. Similarly, the hydrogen bond restricts within motion of the amide group, so that the  $\beta$  peak of PA6 does not appear in the blended sample (PA6-40%). The partial amide group of PA6 and chitosan forms hydrogen bond, decreasing the  $\beta$  peak (PA6-90%). As noted above, the disappearance of the  $\gamma$ ,  $\beta$  and  $\beta_d$  peaks also explained why the PA6-40% displayed excellent miscibility. Generally,  $\alpha$  peak of the blended samples shifts toward lower temperature with increasing PA6 content. The mechanical loss in this stage includes the main chain motion of both PA6 and chitosan and the continuous phase motion among the two compositions, as illustrated in Figure 9. There are two types of hydrogen bond produced between chitosan and PA6. One is the formed between the chitosan and PA6, the other is w-bridge resulted from moisture among the two compositions.

#### Effects of Moisture Permeating into Dried Samples :

From the previous discussion, the moisture is likely to be a cross-linking agent or plasticizer in the wet sample. Currently, no study describes about the action of moisture at certain temperature. Therefore, the sample is placed into a vacuum oven for 10 min at 100 °C to remove the moisture before testing.

Figure 10 displays the relationship between the storage modulus ( $E'$ ) and temperature for the dried samples. At the same ratio, the  $E'$  value of dried sample is lower than that of wet sample below 0 °C and the  $E'$  curves of the dried samples are flatter than that of the wet samples with increasing temperature. In contrast with dried samples, w-bridge results in the high  $E'$  value below 0 °C in wet samples. Comparing the wet and dried samples of PA6-40% in Figure 8 and Figure 10, the

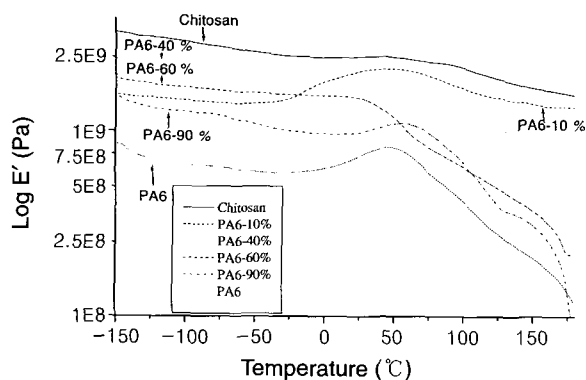


Figure 10. Storage modulus ( $\log E'$ ) of "dried" samples.

modulus of dried sample is  $0.5 E^9 Pa$  which is less than that of wet samples. The phenomenon indicates that the moisture of the wet samples acts as filler or forms a small amount of w-bridge. The moisture can not promote modulus and the modulus only decreases slightly after moisture removal (as PA6-40%). The strong hydrogen bond generates between the chitosan and PA6 in this blend ratio, so that PA6-40% has the highest  $E'$  value in all dried samples. Thus, this sample possibly achieves good miscibility. Comparatively, the  $E'$  value of dried sample differs greatly from that of wet sample below 0 °C for PA6-60%, meaning that PA6-60% wet sample has a large amount of w-bridge. The modulus reduces sharply after removal of moisture.

Heat provides the energy for molecular motion, so that main chain motion occurs at higher temperature and the modulus decreases gradually with increasing temperature. Figure 10 indicates that the modulus of the samples displays a significant increase from 0 to 50 °C, except for PA6-60% and PA6-40%. Moreover, the modulus exceeds that at low temperature for PA6-10% dried sample. Because of the moisture penetrates into the sample again in the temperature range of 0~50 °C, the w-bridge causes the increasing modulus. moisture is difficult to permeate into intermolecular force due to a great hydrogen bond for PA6-40%, so that its modulus is not increased within the temperature range of 0~50 °C. A little moisture entering this blended sample is only attached to the polarity group of PA6 and chitosan without forming w-bridge. Therefore, no modulus increases within this temperature range, explaining the presumably higher miscibility of PA6-40%.

To verify the above observations, DMA testing is conducted on the dried samples under the same conditions. The samples are weighed before DMA testing, and weighed again when the temperature reaches 50 °C. The results of sample weighing demonstrate that samples' weight increases as a result of moisture penetrated into the samples.

Figure 11 illustrates the relationship between the mechanical loss tangent ( $\tan \delta$ ) and the temperature of the dried samples. Below 0 °C, the w-bridge that restricts the molecular chain motion does not exist in the dried samples, and thus the  $\beta$  and  $\gamma$  peaks of the samples should appear. Only PA6-90% displays  $\gamma$  and  $\beta$  peaks for all blended samples from Figure 11. Notably, the temperature of  $\gamma$  peak in PA6-90% is similar to that in PA6. But, the  $\beta$  peak of PA6-90% is located at the higher temperature than that of the  $\beta$  peak of PA6. Moreover, PA6-90% has a small shoulder around -90 °C. This shoulder temperature



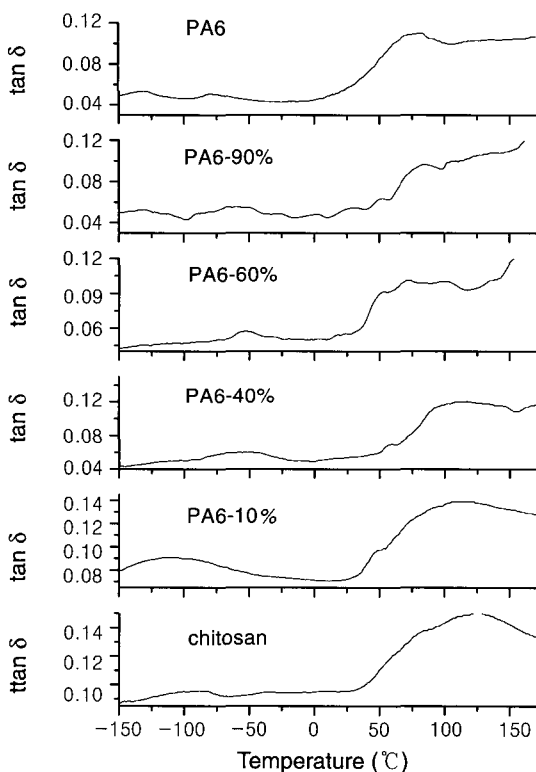


Figure 11. Loss tangent ( $\tan \delta$ ) of “dried” samples.

is close to the  $\gamma$  peak temperature of chitosan. The temperature of the  $\beta$  peak increased because chitosan restricts the partial motion of the amide group in PA6-90%. However, the PA6-40% and PA6-60% samples display a loss peak at around -50 °C and the temperatures for both loss peaks are approximately 20 °C higher than that of the  $\beta$  peak of PA6. Because chitosan and the amide group in PA6 form intermolecular hydrogen bond, the miscibility of chitosan and PA6 increases. Similarly, a loss peak of PA6-10% dried sample appears at -150 ~ -50 °C. This temperature range includes  $\gamma$  and  $\beta$  peaks of PA6 and  $\gamma$  peak of chitosan, demonstrating the interaction between chitosan and PA6 at this temperature range. However, this interaction does not imply that PA6-10% has good miscibility.

The sample gradually absorbs moisture above 0 °C, causing abnormal increase of the modulus and wide  $\alpha$  peak, particularly in chitosan and PA6-10%. This is the result of w-bridge effect, which involves relaxations among composites and between moisture and sample. The results of relaxations also widen  $\alpha$  peak. PA6-40% displays only one  $\alpha$  peak at 85 ~ 103 °C and this peak is slightly narrow compared with chitosan and PA6-10%. Additionally, a shoulder appears around

50 °C. The shoulder probably is formed by intramolecular moisture filler. PA6-60% and PA6-90% have the same phenomenon. Moreover, PA6-60% and PA6-90% present two  $\alpha$  peaks corresponding to the main chain motion in PA6 and chitosan, demonstrating that the two samples have a two-phase structure when moisture exist. The multiple peaks appearing at 0 ~ 100 °C demonstrates that PA6-90% has phase separation. PA6-60% display only one peak at low temperature, but there are several peaks at high temperature. The two-phase of PA6-60% are partially miscible.

**Dynamic Mechanical Properties of Dried Samples in Dry Condition :** To prevent moisture penetrating into dried samples again, a sealed type cooling tank is used to avoid liquid nitrogen bringing moisture into samples. The samples hold for 5 min at 100 °C, and then quench to -150 °C rapidly. The dry nitrogen gas (20 cm<sup>3</sup>/min) is continuously added to the system.

Figure 12 illustrates the relationship between the storage modulus ( $E'$ ) and temperature under above test condition. PA6-10% and PA6-90% display no abnormal increase in modulus from 0 to 50 °C. At higher temperature, the moisture is unable to affect the modulus, and thus their modulus decreases slightly compared with the samples shown in Figure 10. Some samples under unsealed testing condition increase in modulus due to the w-bridge at 0 ~ 50 °C. When the moisture is eliminated, PA6-40% has the highest modulus among all blends, indicating the PA6-40% has the best miscibility in blends as show in Figure 12.

Figure 13 illustrates the relationship between the  $\tan \delta$  and temperature under this test condition. The loss peak at low temperature resembles that in Figure 11, indicating that the dried samples are unaffected by moisture at low temperatures.

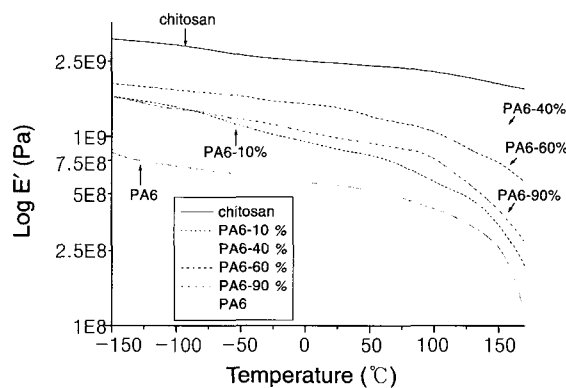


Figure 12. Storage modulus ( $\log E'$ ) of “dried” samples in the dry condition.

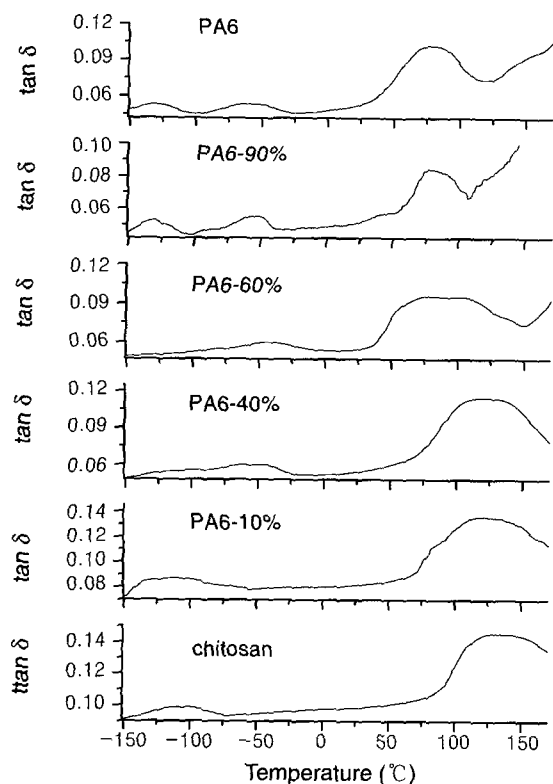


Figure 13. Loss tangent ( $\tan \delta$ ) of "dried" samples in the dry condition.

Since moisture does not exist, the temperature range of the  $\alpha$  peak is narrower than that in Figure 11 and shifts toward high temperature as shown in Figure 13. This investigation finds that the  $\alpha$  peak of the blends shifts toward high temperature with increasing chitosan content. This phenomenon is attributed to the hydrogen bond generated between chitosan and PA6. This hydrogen bond restricts the molecular chain motion and makes  $\alpha$  peak to shift toward high temperature. Comparison between Figures 13 and 11 reveals that the shoulder around 50 °C disappears, explaining that the shoulder is precisely caused by the moisture filler in the samples.

From Figure 13, three loss peaks of PA6 ( $\gamma$ ,  $\beta$  and  $\alpha$  peaks) are laid on -130, -62 and 78 °C, respectively. The  $\beta$  peak of PA6-90% shifts toward high temperature and narrows, and a shoulder appears at the low temperature that corresponds to the  $\gamma$  peak of chitosan. The  $\alpha$  peak of PA6-90% shifts to high temperature slightly, but a shoulder appears around 100 °C, indicating that chitosan and PA6 are partially miscible. The same situation occurs in the PA6-60%, for which the  $\alpha$  peak is located in 53~108 °C and composes of the  $\alpha$  peak of PA6 and chitosan, demonstrating that PA6-60% also has the phase

separation.

The two peaks of the PA6-10% appear, corresponding to the  $\gamma$  and  $\alpha$  peaks of chitosan. A shoulder of PA6-10% appears around 80 °C that corresponds to the  $\alpha$  peak of PA6, indicating individually molecule chain motion of PA6 and chitosan and the existence of phase separation. PA6-40% displays only one peak that approaches the  $\beta$  peak of PA6 at low temperature. Additionally, chitosan causes the  $\alpha$  peak to shift toward high temperature, ranging from 105 to 140 °C, and the shoulder at high temperature is absence. To sum up, PA6-40% has the highest miscibility in all blended samples.

#### 4. Conclusions

The FT-IR spectra demonstrated the hydrogen bond between chitosan and PA6. Hydrogen bond and moisture were two major factors in modulus and miscibility for chitosan, PA6 and the blended samples. moisture was dissipated near 0 °C, causing rapidly reducing modulus. Over 0 °C, moisture within free volumes penetrated into the intermolecular spacing and formed w-bridge, increasing the modulus. For dried samples, the  $\beta$ d peak disappeared around 0 °C, verifying that moisture is a major reason for the sharp modulus decline at low temperatures. Under unsealed test conditions, some samples with low miscibility formed the w-bridge over 0 °C due to moisture penetrating into the PA6 and chitosan molecule chain, causing significant modulus increase. The moisture filler brought about a shoulder around 50 °C, and the shoulder existed in several blended samples. moisture significantly affects the storage modulus of high hydrophilic chitosan/PA6 blended samples. Following the w-bridge formed, the storage modulus clearly increased. The w-bridge also influenced molecular chain motion and widened  $\alpha$  peak. Miscibility in this work was considered first in blend application and manufacturing. This investigation found that PA6-40% had the best miscibility in the all blends.

#### References

1. W. F. Lee and Y. M. Tu, *J. Appl. Polym. Sci.*, **76**, 170 (2000).
2. J. Hosokawa, M. Nishiyama, K. Yoshihara, T. Kubo, and A. Terabe, *Ind. Eng. Chem. Res.*, **30**, 788 (1991).
3. T. Kondo, C. Sawatari, R. St. John Manley, and D. Gray, *Macromolecules*, **27**, 210 (1994).
4. J. F. Masson and R. St. John Manley, *Macromolecules*, **24**, 6670 (1991).

5. Y. Nishio, T. Haratani, T. Takahashi, and R. St. John Manley, *Macromolecules*, **22**, 2547 (1989).
6. Y. Nishio and R. St. John Manley, *Polym. Eng. Sci.*, **30**, 71 (1990).
7. Y. Nishio and R. St. John Manley, *Macromolecules*, **21**, 1270 (1988).
8. Y. Nishio, S. K. Roy, and R. St. John Manley, *Polymer*, **28**, 1385 (1987).
9. M. Hasegawa, A. Isogai, F. Onabe, M. Usuda, and R. Atalla, *J. Appl. Polym. Sci.*, **45**, 1873 (1992).
10. Shalaby W. Shalaby, *Biomedical Polymers*; Carl Hanser Verlag, Munich Vienna New York, 1994.
11. S. Bartnicki-Garcia and W. J. Nickerson, *Biochim. Biophys. Acta.*, **5**, 102 (1962).
12. T. D. Rathke and SM. J. Hudson, *Macromol. Sci. Rev. Macromol. Chem. Phys.*, **C34**, 375 (1994).
13. T. Hol, *Bioindustry*, **8**, 102 (1997).
14. L. U. Fung, *Bioindustry*, **9**, 27 (1998).
15. P. J. Flory, *Principles of Polymer Chemistry*, Cornell University, New York, 1953.
16. R. H. Boyd and P. J. Phillips, *The Science of Polymer Molecules*, Cambridge, New York, Cambridge University Press, 1993.
17. V. Gonzalez, C. Guerrero, and U. Ortiz, *J. Appl. Polym. Sci.*, **78**, 850 (2000).
18. K. Sreenivasan, *Polym. Degrad. Stab.*, **52**, 85 (1996).
19. S. A. Bradley and S. H. Carr, *J. Polym. Sci., Phys. Ed.*, **14**, 111 (1976).
20. R. J. Samuels, *J. Polym. Sci., Phys. Ed.*, **19**, 1081 (1981).
21. E. Fukada and S. Sasaki, *J. Polym. Sci., Phys. Ed.*, **13**, 1845 (1975).
22. K. Nishinari, D. Chatain, and C. Lacabanne, *J. Macromol. Sci. Phys.*, **B22**, 529(1983).
23. M. Kakizaki, H. Yamamoto, T. Ohe, and T. Hideshima, in *Chitin and Chitosan*, G. Skjak-Break, T. Anthonsen, and P. Sandford, Editors, Elsevier, London, 1989.
24. R. A. A. Muzzarelli, C. Jeuniaux, and G. W. Gooday (Eds.), *Chitin in Nature and Technology*, Plenum, New York, 1986.
25. I. Vieira, V.L.S. Severgnini, D.J. Mazera, M.S. Soldi, E.A. Pinheiro, A.T.N. Pires, and V. Soldi, *Polym. Degrad. Stab.*, **74**, 151 (2001).
26. G. Cardenas, J. C. Paredes, G. Cabrea, and P. Casals, *J. Appl. Polym. Sci.*, **86**, 2742 (2002).
27. C. Peniche-Covas, W. Arguelles-Monal, and J. S. Roman, *Polym. Degrad. Stab.*, **39**, 21 (1993).
28. N. M. Langer and C. A. Wilkie, *Polym. Adv. Technol.*, **9**, 290 (1998).
29. D. A. Costa and C. M. F. Oliveira, *J. Appl. Polym. Sci.*, **81**, 2556 (2001).
30. X. Qu, A. Wirsén, and A. Albertsson, *Polymer*, **41**, 4841 (2000).
31. P. Gijssman, R. Steenbakkens, C. Furst, and J. Kersjes, *Polym. Degrad. Stab.*, **78**, 219 (2002).
32. H. Bockhorn, A. Horung, U. Horung, and J. Weichmann, *Thermochimica Acta*, **337**, 97 (1999).
33. M. Pizzoli, G. Ceccorulli, and M. Scandola, *Carbohydrate Research*, **222**, 205 (1991).
34. D. C. Prevorsek, R. H. Butler, and H. K. Reimschuessel, *J. Polym. Sci., Pt. A-2*, **9**, 867 (1971).
35. M. Takayanagi, *Mem. Fac. Eng. Kyushu Univ.*, **23**, 1 (1963).
36. J. A. Ratto, C. C. Chen, and R. B. Blumstein, *J. Appl. Polym. Sci.*, **59**, 1451 (1996).